American Mineralogist, Volume 74, pages 1186–1194, 1989

Magnetoplumbite, $Pb^{2+}Fe^{3+}_{12}O_{19}$: Refinement and lone-pair splitting

Paul Brian Moore
Department of the Geophysical Sciences, The University of Chicago, Chicago, Illinois 60637, U.S.A.
Pradip K. Sen Gupta
Department of Geology, Memphis State University, Memphis, Tennessee 38152, U.S.A.
Yvon Le Page
National Research Council, Ottawa, Ontario K1A 0R6, Canada

Abstract

Synthetic magnetoplumbite, $Pb^{2+}Fe^{3+}_{12}O_{19}$, hexagonal holosymmetric, $a = 5.873(2)$, $c = 23.007(6)$ Å, space group $P6_3/mmc$, $Z = 2$, $D_{calc} = 5.71$ g·cm^{-3} has been defined to $R = 0.041$ ($MoK\alpha_1$) with the use of 397 unique F_o values. The structure is based on ten oxygen layers parallel to {0001} of the close-packed stacking sequence [·*chhhcchhhc*·]. Alternatively, it could be written *RSR'S'*, primes connoting layers resulting from the $\{6_3\}$ screw operation, $R = (hhh)$ or $[PbFe_6O_{11}]^{2-}$, $S = (cc)$ or $[Fe_6O_8]^{2+}$.

Bond-distance averages are $^{[6]}$Fe(1)–O 1.998, $^{[4]}$Fe(2)–O 1.942, $^{[4]}$Fe(3)–O 1.888, $^{[6]}$Fe(4)–O 2.007, $^{[6]}$Fe(5)–O 2.017, and $^{[12]}$Pb–O 2.90 Å. The nine nonequivalent Pb–O distances range from 2.64 to 3.24 Å.

Both Fe(2) and Pb sites are disordered. The disordering of the latter, believed to be the consequence of a lone pair–bond pair interaction, is striking. The Pb centroid converged to (12*j*) (0.720, 0.384, ¼), displaced $\Delta = 0.31$ Å from the invariant point (2*d*) (⅔, ⅓, ¼), each (12*j*) point on the average ⅙ occupied. The Pb–Pb$^{(10)}$ 0.61-Å distance is a pseudo-inversion and corresponds to similar values for other split Pb^{2+} oxysalts. The cations Pb and Fe(1) to Fe(5) are related to the centroids of the metals in $6CeNi_3$ intermetallic.

A *splitting index, P,* is defined as the ratio of the number of elements [*p*(a)] of the split Wyckoff atom position to the number of elements [*p*(b)] of the coalesced position of lower order, that is, $P = |p(a)|/|p(b)|$. For magnetoplumbite with $2d \rightarrow 12j$, the splitting index is $P = 12/2 = 6$.

Introduction

Magnetoplumbite, $Pb^{2+}Fe^{3+}_{12}O_{19}$, is one of several true ferrite (Fe^{3+}) phases that have gained considerable importance as permanent magnets. Natural material is an early skarn mineral, practically confined to Långban, Värmland, Sweden, where it was locally formerly abundant in association with manganophyllite mica and several other early lead oxysalts such as hedyphane and kentrolite-melanotekite. The natural mineral, usually of complex composition owing to other subordinate components as MnO, Mn_2O_3, Al_2O_3, and TiO_2, was early known as a strongly magnetic mineral even though no Fe^{2+} was present. Hence, it is one of the many known hexagonal ferrites that have been subsequently grown as synthetic crystals. Magnetoplumbite was first christened and described by Aminoff (1925).

Our interest in magnetoplumbite concerns Pb^{2+} and its crystallochemical behavior. Several recent studies focused on anomalous behavior of Pb^{2+} in oxysalt minerals that crystallized at relatively high temperature. Considerable structure study has been bestowed upon $BaFe^{3+}_{12}O_{19}$, which is isotypic to magnetoplumbite, $PbFe^{3+}_{12}O_{19}$. To our knowledge, no structure refinement has been bestowed upon the Pb^{2+} salt. As the Pb^{2+} cation has a lone pair of electrons, that is $6s^2Pb^{2+}$ or $Pb^{2+}\psi$, whereas the Ba^{2+} cation has no valence electrons, a chemical crystallographic comparison is desirable between the two ferrites of magnetoplumbite structure type.

Experimental details

Natural magnetoplumbites are notoriously "dirty," containing at least five components in varying degrees of solid solution. Mr. John S. White, Jr., of the U.S. Natural History Museum (Smithsonian Institution) sent the senior author some synthetic crystals of NMNH 136741. The crystals were flux grown, and Dr. Kurt Nassau of Bell Labs informed us that the initial temperature was 1000 °C and the crystals were grown by slow cooling. We checked our sample on the electron microprobe. Pb and Fe were the only elements detected, and their ratio corresponded to a magnetoplumbite composition. A crystal was then ground into a sphere, cursorily checked on the diffractometer, and deemed suitable for data collection. Twenty-five reflections in the range $24° < 2\theta < 36°$ determined the orientation matrix and refined structure cell data. The experimental details, summarized in Table 1, are standard but will be defined further in the text if necessary. Neutral-atom scattering factors and real and

0003–004X/89/0910–1186$02.00

imaginary dispersion corrections were taken from Ibers and Hamilton (1974).

Refinement proceeded from the initial coordinates of Townes et al. (1967) ($R = 0.059$ for their $BaFe_{12}O_{19}$). Two central problems presented themselves in our study. The M(2) site, noted in earlier work, is not ordered at its invariant point (0, 0, ¼). This, in turn, affects apical bonded oxygen O(1) and its equatorial oxygen O(3). A far more difficult problem was Pb, the central quest of our study. It, too, was disordered, split from its (2*d*) invariant position (⅔, ⅓, ¼) to (12*j*) at (*x*, *y*, ¼), with each point 1/6 occupied. In the next section, these anomalies will be discussed in detail. Briefly, several models were tried including Fe(2) at (0, 0, ¼), Pb at (⅔, ⅓, ¼), Fe(2) at (0, 0, *z*), and Pb at (*x*, *y*, ¼).

Table 1a lists the observed and calculated structure factors of the present study.[1]

Chemical crystallography

The most detailed and extended discussion on the hexagonal ferrite $BaFe_{12}O_{19}$ of magnetoplumbite structure type was offered by Obradors et al. (1985). Their study led to $R = 0.016$ for a split Fe(2) site and anisotropic thermal motion of all atoms. They conceived the structure built of blocks, *R* and *S*. *R* corresponds to the (*hhh*) sequence with composition $[BaFe_6O_{11}]^{2-}$ and *S* corresponds to the (*cc*) sequence or the spinel layer $[Fe_6O_8]^{2+}$. Thus, *RSR'S'* is the *c*-axis repeat with primes connoting layers resulting from the $\{6_3\}$ screw operation.

Other recent studies with good convergence include Townes et al. (1967), $BaFe_{12}O_{19}$, $R = 0.059$; and Grey et al. (1987) on natural ca. $Ba[Ti_3Cr_4Fe_4Mg]O_{19}$, $R = 0.044$. We shall focus on the Obradors et al. (1985) study.

The magnetoplumbite structure is based on principles of crystallographic close-packing where 38 anions [38ϕ: 4O(1) + 4O(2) + 6O(3) + 12O(4) + 12O(5)] and 2ϕ' cations [$2Pb^{2+}$] make up the close-packed sequence of 10 layers in the unit cell. With 4ϕ per layer, eight oxygen layers occur, the remaining two layers each made up of $3\phi + \phi' = 3O + 1Pb$. The 24 small cations in the cell, Fe^{3+}, consist of 18 in octahedral coordination and 6 in tetrahedral coordination. Of the latter, two are disordered at M(2), exactly half-occupied in the (4*e*) Wyckoff position. This position for M(2) required special attention. All other Fe^{3+} cation positions exhibited normal behavior.

An interesting part of the crystal structure is the close-packed ϕ-layers, which are based on the sequence [·*chhhcchhhc*·]. Note the sequence is doubled to satisfy the $\{6_3\}$ rototranslation in $P6_3/mmc$. In this sequence, the origin of the unit cell is at the first period, an inversion center that appears everywhere along [0001] between the cubic close-packed sequence *cc*. The mirror planes normal to the *c* axis occur at $z = ¼, ¾$; these coordinates are identical with the central "*h*" in the triad *hhh* of hexagonal close-packing. This 10-layer sequence leads to $c/10 = 2.30$ Å, a typical layer translation in dense-packed ferrite and aluminate structures. Hematite, α-Fe_2O_3, has the same layer translation. The symmetry group forces three unique cation layers: one is at $z \approx 0$ (and ½) for M(1) and M(3), the second at $z \approx ⅛$ (and ⅜, ⅝, ⅞) for M(5), and the third at $z \approx ¼$ (and ¾) for M(2), M(4), and Pb. The first layer is based on a glaserite-type pinwheel or the (3 + 3)*c* module (Moore, 1973) that creates the sheet with cell stoichiometry

$$^{[6]}M(2)_2{}^{[4]}M(3)_4\phi_{16[=4O(2)+12O(4)]}.$$

The second layer is an octahedral sheet of spinel type (111) layers, with cell stoichiometry

$$^{[6]}M(5)_{12}\phi_{32[=4O(1)+4O(2)+12O(4)+12O(5)]} = {}^{2}_{\infty}M_3\phi_8.$$

These two layers each condense through corner and edge sharing in the {0001} plane and between these planes.

The third layer centered at $z = ¼$ is the most remarkable and shows extensive cation disorder. The remaining cations M(2), M(4), and Pb reside here, of which M(2) and Pb are disordered. The octahedrally coordinated M(4) cation fuses with another octahedron by face-sharing at $z = ¼, ¾$ to form the $M(4)_2O(3)_3O(5)_6 = M_2\phi_9$ dimeric octahedral cluster as found in hematite, α-Fe_2O_3. In hematite, the Fe–Fe' distance of 2.90 Å across a shared face contrasts with magnetoplumbite's M(4)–M(4)' distance of 2.75 Å across a similar shared face in the dimer. The difference of $\Delta = 0.15$ Å between the two compounds probably has some electrostatic explanation based on structure type. The M(2) site presented a long problem in

Table 1. Experimental details for magnetoplumbite

(A) Crystal-cell data	
a (Å)	5.873(2)
c (Å)	23.007(6)
V (Å^3)	687.2(1)
Space group	$P6_3/mmc$, hexagonal
Z	2
Formula	$PbFe_{12}O_{19}$
D_{calc} (g·cm^{-3})	5.71
μ (cm^{-1})	246.9
μR	3.70
(B) Intensity measurements	
Crystal size	Sphere, $R = 150$ μm
Diffractometer	Enraf-Nonius CAD4
Monochromator	Graphite
Radiation	Mo$K\alpha_1$
Scan type	θ–2θ
2θ range	0.5–60°
Reflections measured	1724
Unique reflections $> 2\sigma F_o$	397 F_o used in refinement
Transmission factor range	0.71–2.41
Secondary extinction coefficient	$4.6(5) \times 10^{-2}$
(C) Refinement of the structure	
R 0.041	$R = \Sigma(\lvert\lvert F_o\rvert - \lvert F_c\rvert\rvert)/\Sigma F_o$
R_w 0.040	$R_w = [\Sigma_w(\lvert F_o\rvert - \lvert F_c\rvert)^2/\Sigma_w F_o^2]^{1/2}$, $w = \sigma^{-2}(F)$
Variable parameters	45
"Goodness of fit" (GOF)	6.22

[1] A copy of Table 1a may be ordered as Document AM-89-415 from the Business Office, Mineralogical Society of America, 1625 I Street, N.W., Suite 414, Washington, D.C. 20006, U.S.A. Please remit $5.00 in advance for the microfiche.

TABLE 2. Magnetoplumbite and $CeNi_3$ intermetallic: Atomic coordinate parameters

Atom	W	P	CN	x	y	z	Δ (Å)	B_{eq}	$(B_{eq})_{Ob}$
Pb	12*j*	1/6	12	0.720(5)	0.384(5)	1/4	0.31	1.50(5)	0.57(1)
Ni(3)	2*d*	1	—	2/3	1/3	1/4			
M(1)	2*a*	1	6	0	0	0	0.00	0.49(8)	0.41(1)
Ni(1)	2*a*	1	—	0	0	0			
M(2)	4*e*	1/2	4 + 1	0	0	0.2559(14)	0.14	0.60(5)	0.43(1)
Ni(2)	2*b*	1	—	0	0	1/4			
M(3)	4*f*	1	4	1/3	2/3	0.02733(9)	0.33	0.42(6)	0.42(1)
Ce(2)	4*f*	1	—	1/3	2/3	0.0418			
M(4)	4*f*	1	6	1/3	2/3	0.19019(9)	1.38	0.51(6)	0.46(1)
Ce(1)	2*c*	1	—	1/3	2/3	1/4			
M(5)	12*k*	1	6	0.1687(1)	−*x*	−0.10881(5)	0.53	0.47(4)	0.47(1)
Ni(4)	12*k*	1	—	0.1666	−*x*	−0.1272			
O(1)	4*e*	1		0	0	0.1511(4)		0.60(3)	0.61(5)
O(2)	4*f*	1		1/3	2/3	−0.0546(4)		0.40(3)	0.48(5)
O(3)	6*h*	1		0.1839(10)	−*x*	1/4		1.01(15)	0.66(5)
O(4)	12*k*	1		0.1565(6)	−*x*	0.0524(2)		0.47(18)	0.56(3)
O(5)	12*k*	1		0.5035(7)	−*x*	0.1499(2)		0.51(19)	0.68(3)

Note: Cations of magnetoplumbite and $CeNi_3$ intermetallic are compared. Atom label, Wyckoff position (*W*), population (*P*), coordination number of oxide anions around cation (CN), atom coordinates (*x*, *y*, *z*), difference in Å between oxide and intermetallic (Δ), and equivalent isotropic thermal parameters for this study (B_{eq}) and Obradors et al. (1985) [$(B_{eq})_{Ob}$] are listed. Standard errors in parentheses refer to the last digit.

magnetoplumbite's chemical-crystallographic history. Earlier studies placed M(2) on the mirror plane at $z = 1/4$, but Townes et al. (1967) gave $z = 0.2567$; Obradors et al. (1985) reported $z = 0.2573$; Grey et al. (1987) reported $z = 0.2571$ for complex, highly substituted, natural $Ba[Ti_3Cr_4Fe_4Mg]O_{19}$; we got $z = 0.2559$ for our synthetic $Pb[Fe_{12}O_{19}]$. A trigonal bipyramid is split into two adjacent tetrahedra sharing the common face at $z = 1/4$, and the M(2) site is on average exactly half-populated. That is, $(2b)(0, 0, 1/4) \rightarrow (1/2 \times 4e)(0, 0, z)$. The difference among z values in the four studies is no more than 0.03 Å. This splitting has been extensively discussed in the earlier papers. Briefly, what results from the trigonal bipyramidal model at $z = 1/4$ is a large isotropic thermal parameter for Fe(2) and marked elongation of the U_{33} component in the anisotropic parameters. Obradors et al. (1985) concluded on the basis of their superior refinements and previous Mössbauer spectroscopy studies that the disorder is a *dynamical* one with Fe(2) oscillating between the two adjacent tetrahedral centroids through the O(3) triangle on the mirror plane.

TABLE 3. Magnetoplumbite: Anisotropic thermal-vibration parameters (×10⁴)

	U_{11}	U_{22}	U_{33}	U_{12}	U_{13}	U_{23}
Pb	218(65)	115(53)	229(7)	68(44)	0	0
Fe(1)	70(9)	U_{11}	45(14)	$1/2U_{11}$	0	0
Fe(2)	104(11)	U_{11}	26(117)	$1/2U_{11}$	0	0
Fe(3)	60(6)	U_{11}	38(8)	$1/2U_{11}$	0	0
Fe(4)	76(7)	U_{11}	43(9)	$1/2U_{11}$	0	0
Fe(5)	72(5)	90(10)	48(5)	$1/2U_{22}$	2(2)	$2U_{13}$
O(1)	113(34)	U_{11}	15(44)	$1/2U_{11}$	0	0
O(2)	56(30)	U_{11}	52(44)	$1/2U_{11}$	0	0
O(3)			Isotropic, $U = 128(18)$			
O(4)	61(20)	71(48)	63(24)	$1/2U_{22}$	3(11)	$2U_{13}$
O(5)	63(20)	35(48)	48(24)	$1/2U_{22}$	7(12)	$2U_{13}$

Note: The U_{ij} values are coefficients in the expression $\exp[-\Sigma_{ij}U_{ij}h_ih_j]$. Estimated standard errors refer to the last digit, and identities are noted.

The most interesting part, and the raison d'être for this study, is the prediction by the senior author that the Pb^{2+} position at purported (2/3, 1/3, 1/4), point symmetry $\{\bar{6}m2\}$ with *no* degrees of freedom, would be split among several sites, removed somewhat from the fixed point. The synthetic crystal, flux grown at initial 1000 °C, was an ideal candidate to test this prediction. Free from impurities, it would minimize possible conflicting conclusions obtained from a chemically complex, natural crystal. Pb occupies an "anion" position in the crystal structure, and its immediate neighborhood is h.c.p. The coordination polyhedron is $Pb[O(3)_6O(5)_6]$ or $Pb\phi_{12}$. The 6O(3) atoms are on the mirror plane at $z = 1/4$ and roughly define an hexagonal outline. The 3O(5) above and 3O(5) below define by themselves a trigonal prism. The polyhedron has $N_0 = 12$ vertices, $N_1 = 24$ edges, and $N_2 = 8$ triangles + 6 squares = 14 faces. Belonging to the $D_{3h} = \bar{6}m2$ = ditrigonal-dipyramidal class, it is generated by rotating the bottom half of the cuboctahedron (ABC = cubic sequence) $\pi/3$ radians at its equator to form the ABA (= hexagonal sequence).

Magnetoplumbite and $CeNi_3$ intermetallic

A remarkable relation of all six cations exists between magnetoplumbite and all atoms in the intermetallic $6CeNi_3$, $a = 4.98(2)$, $c = 16.54(6)$, $c/a = 3.321$, space group $P6_3/mmc$. The intermetallic was investigated in considerable detail (Mo$K\alpha$ radiation, 769 F_o) by Cromer and Olsen (1959). The $CeNi_3$ structure type embraces at least 28 other phases listed in Villars and Calvert (1985). It consists of alternating single layers of $CeNi_5$ ($CaCu_5$ type) and double layers of $CeNi_2$ ($MgCu_2$ type). The cell of magnetoplumbite has 26 cations or Pb_2Fe_{24}, but the intermetallic has 24 atoms or Ce_6Ni_{18}.

The coordinates of $CeNi_3$ are listed below the cation coordinates for magnetoplumbite in Table 2. The match is good between five of the six unique pairs, the difference Δ (scaled to the magnetoplumbite cell) being less than 0.53 Å. The big difference is for the remaining pair (4*f*)Fe(4) − (2*c*)Ce(1) where $\Delta = 1.38$ Å, one atom effectively being split into two by interleaving anions. This corresponds to the $Fe(4)_2O_9$ face-sharing dimer. The magnetoplumbite structure can be conceived as a lamination along [0001] of alternating cation (metal) and oxide layers. In fact, $c/a = 3.917$ for magnetoplumbite, an expansion along *c* of over 15% relative to $CeNi_3$. Such dilations as a consequence of anion insertion in intermetallics were discussed in considerable detail by Moore et al. (1989).

Table 3 presents the anisotropic thermal-vibration ellipsoids for magnetoplumbite. These data are good means of assessing not only crystal quality but also comparing different members of a structure type. We converted the β_{ij} values of Obradors et al. (1985) into a parallel set for comparison. For Fe(1), Fe(3), Fe(4), Fe(5), O(2), and O(4), the match is quite satisfactory. The contrast between the disordered cations Pb and Fe(2), however, is noteworthy—as is the contrast where they are bonded to O(1), O(3), and O(5). In fact, O(3) was constrained to refine in isotropic mode, the anisotropic thermal parameters always yielding nonpositive definite solutions. This is the only anion receiving bonds from *both* disordered cations. Anisotropic thermal vibration demonstrates yet again the utility of these distortions in assessing disorder in crystals when compared for one structure type. Finally, the Pb parameters, although large, are neither nonpositive nor severely distorted in (⅙ × 12*j*) (*x*, *y*, ¼), quite unlike our early results in (⅓ × 6*h*)(*x*, $\bar{x}$, *z*): on the (6*h*) position, the Pb atoms invariably split off the vertical mirror plane.

The Pb anomaly

Figure 1 features the M(2), M(4), Pb, O(1), O(3), O(5) at $z = ¼$. For $Pb\phi_{12}$, six triangular faces are shared with M(4) above and below, all six O(5)–O(5)′ edges above and below are shared with the $Fe(5)_3\phi_8$ sheet above and below, and three O(3)–O(3)′ edges on the mirror plane associated with the squares are shared with $M(2)\phi_4$. This means that all 12 vertices, all 24 edges, and 6 of the 14 faces are shared. The edges are noted accordingly in Table 4, which lists bond lengths and angles. Pb, however, exhibits anomalous behavior, and the phase in this study is the first reported example of a magnetoplumbite phase displaying such a phenomenon. Rather than remaining fixed (invariant) at (⅔, ⅓, ¼), it is split into six pieces, each piece ⅙ occupied on average. Our converged site is (0.720, 0.384, ¼), and its displacement from the invariant point is $\Delta = 0.31$ Å. This displacement leads to a range of Pb–Pb′ and Pb–O(3,5) distances, from 0.28 to 0.61 Å for the former and from 2.64 to 3.24 Å for the latter. Note that the maximal Pb–$Pb^{(10)}$ 0.61-Å separation, a pseudo-inversion, closely matches values found in joesmithite ($\Delta = 0.60$ Å) and KPS ($\Delta = 0.59$ Å). In fact, $Pb^{(10)}$ ($\bar{y}$, $\bar{x}$, *z* applied to coordinates in Table 2) is (0.616, 0.280, ¼). The inversion, which does not exist in ($\bar{6}m2$), of Pb through (⅔, ⅓, ¼) would give $Pb^{(i)}$ (0.614, 0.282, ¼), $Pb^{(10)}$ and $Pb^{(i)}$ being within the limit of error for the coordinate refinement of Pb. This suggests that splitting proceeds $\{1\}\cdot\{\bar{1}\}\cdot\{3\}$ or $1\cdot2\cdot3 = 6$. That is, sixfold splitting of Pb can occur merely through the operation of inversion, all elements of symmetry in $P6_3/mmc$ remaining unchanged. These and other compounds are compared later.

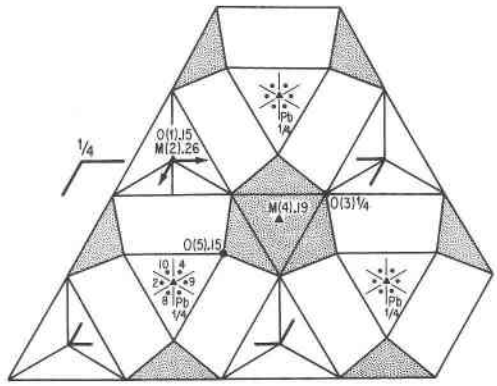

Fig. 1. Magnetoplumbite: disordered sheet of Fe(2) and Pb at $z = ¼$. Symmetry-equivalent split Pb centroids are denoted by numbers (cf. Table 5). Some elements of symmetry are shown.

Perhaps the most convincing evidence for this remarkable lone-pair effect by $6s^2Pb^{2+}$ can be demonstrated by deliberately controlled refinement. We summarize four such refinements:

(a) Convergence involving all conventional variable parameters, full-matrix anisotropic refinement. The results are tabulated in this study; $R = 0.041$, $B_{eq} = 0.60(5)$ Å² for M(2), $B_{eq} = 1.50(5)$ Å² for Pb.

(b) Output from (a) but $z = ¼$ for M(2). Convergence led to $R = 0.043$, $B_{eq} \approx 1.17$ Å² for M(2), $B_{eq} \approx 1.6$ Å² for Pb.

(c) Output from (a) but $z = ¼$ for M(2) and *isotropic* refinement for all atoms. $R = 0.065$ and $B_{eq} \approx 1.5$ Å² for Pb.

(d) Output from (a) but $z = ¼$ for M(2), Pb *fixed* at (⅔, ⅓, ¼), and isotropic refinement for all atoms. $R = 0.156$ and $B_{eq} \approx 3.8$ Å² for Pb.

A lone-pair effect

It is believed that the anomalous behavior of $6s^2Pb^{2+}$—its splitting into six equivalent pieces each ⅙ occupied—is the basis for anomalous chemical-crystallographic behavior of $Pb[Fe_{12}O_{19}]$ or true magnetoplumbite. Several clues suggest that $R = 0.041$ is indeed a good convergence for this compound. First, $B_{eq} = 1.50$ Å² for Pb is way out of line with $B_{eq} = 0.57$ Å² for its Ba equivalent (Obradors et al., 1985). Ba^{2+} as an ion has no remaining valence electrons; Pb^{2+} has one $6s^2$ lone pair of electrons remaining.

A second compelling argument arises when Pb is fixed

TABLE 4. Magnetoplumbite: Fe–O bond distances (Å) and angles (°)

	Fe(1)	
		OB
6 Fe(1)–O(4)	1.998(2)	2.000
average	1.998	2.000
		O–Fe–O′
6 O(4)–O(4)$^{(2)*}$	2.758(9)	87.3(2)
6 O(4)–O(4)$^{(3)}$	2.891(10)	92.7(2)
average	2.824	90.0
	Fe(2)	
3 Fe(2)–O(3)	1.876(2)	1.867
1 Fe(2)–O(1)	2.139(3)	2.128
[1 Fe(2)–O(1)$^{(12)}$	2.410(3)	2.468]
average	1.942	1.932
3 O(1)–O(3)	2.945(8)	85.9(10)
3 O(3)–O(3)$^{(4)}$	3.241(15)	119.5(3)
average	3.093	102.7
	Fe(3)	
1 Fe(3)–O(2)	1.885(9)	1.894
3 Fe(3)–O(4)	1.889(2)	1.894
average	1.888	1.894
3 O(2)–O(4)	3.049(8)	107.8(2)
3 O(4)–O(4)$^{(4)}$	3.115(10)	111.1(2)
average	3.082	109.5
	Fe(4)	
		OB
3 Fe(4)–O(5)	1.964(3)	1.969
3 Fe(4)–O(3)	2.050(1)	2.073
average	2.007	2.021
3 O(3)–O(3)$^{(2)**}$	2.633(15)	79.9(2)
6 O(3)$^{(2)}$–O(5)	2.825(6)	89.4(2)
3 O(5)–O(5)$^{(2)}$	2.998(11)	99.5(2)
average	2.820	89.6
	Fe(5)	
2 Fe(5)–O(5)$^{(6)}$	1.916(4)	1.932
1 Fe(5)–O(1)$^{(1)}$	1.973(5)	1.985
1 Fe(5)–O(2)	2.088(6)	2.092
2 Fe(5)–O(4)$^{(3)}$	2.104(4)	2.114
average	2.017	2.028
2 O(2)–O(5)$^{(6)*}$	2.750(8)	86.6(2)
1 O(4)$^{(3)}$–O(4)$^{(5)*}$	2.758(10)	81.9(2)
2 O(1)$^{(1)}$–O(4)$^{(3)*}$	2.773(8)	85.6(2)
2 O(4)$^{(3)}$–O(5)$^{(6)}$	2.853(6)	90.3(2)
2 O(1)$^{(1)}$–O(5)$^{(6)}$	2.937(4)	98.1(2)
2 O(2)–O(4)$^{(3)}$	2.939(4)	89.0(2)
1 O(5)$^{(6)}$–O(5)$^{(7)}$	2.998(11)	97.2(2)
average	2.855	89.9

Note: Under each atom heading are listed bond distances and angles. Estimated standard errors refer to the last digit. The Fe–O distances of Obradors et al. (1985) are appended under OB.

* Shared edges between polyhedra. Equivalent points refer to Table 2 and appear as superscripts in parentheses: (1) $-x, -y, -z$; (2) $y-x, -x, z$; (3) $x-y, x, -z$; (4) $-y, x-y, z$; (5) $y, y-x, -z$; (6) $-x, y-x, -z$; (7) $x-y, -y, -z$; (8) $x, x-y, z$; (9) $y-x, y, z$; (10) $-y, -x, z$; (11) $y, x, -z$; (12) $x, y, \frac{1}{2}-z$.

** Edges of shared face between polyhedra.

at invariant (⅔, ⅓, ¼). Here, the B_{eq} blew up to 3.8 Å^2, and $R = 0.16$ was the convergence. A third telling example is found in the Pb–O distances. Six *unique* Pb–O equatorial distances and three *unique* apical distances exist. In Ba[$Fe_{12}O_{19}$], only six *equivalent* Ba–O equatorial distances and six *equivalent* apical distances exist. That is, for Pb[$Fe_{12}O_{19}$] compared with Ba[$Fe_{12}O_{19}$], nine unique Pb–O distances exist in the former compared with two unique Ba–O distances in the latter. Finally, large estimated standard deviations in unique Pb–Pb′ distances (±0.05 Å) suggest that such a splitting is not so simple as subdivision into six pieces (atomic number of ⅙Pb ≈ 14 electrons) but that the refined *x, y,* ¼ centroid for Pb^{2+} may be merely an averaged value over many site points that converge upon it.

TABLE 5. Magnetoplumbite: Pb–Pb′ and Pb–O distances (Å)

	Pb–Pb′	
	Pb–Pb$^{(8)}$	0.28(7)
	Pb–Pb$^{(9)}$	0.33(7)
	Pb–Pb$^{(2)}$	0.53(4)
	Pb–Pb$^{(4)}$	0.53(4)
	Pb–Pb$^{(10)}$	0.61(5)
	Pb–O	
Apical	2 Pb–O(5)$^{(2)}$	2.69(1)
	2 Pb–O(5)	2.86(2)
	2 Pb–O(5)$^{(4)}$	3.00(2)
	average	2.85
Equatorial	Pb–O(3)^{t}	2.64(2)
	Pb–O(3)$^{(4)t}$	2.77(3)
	Pb–O(3)$^{(2)t}$	2.83(3)
	Pb–O(3)$^{(4)}$	3.10(3)
	Pb–O(3)$^{(2)}$	3.11(3)
	Pb–O(3)	3.24(2)
	average	2.95
	all Pb–O	2.90

Note: See Table 4 for designations. Superscript "t" corresponds to cell translation.

Therefore, $R = 0.041$ is considered an acceptable convergence for the problem at hand. Our magnetoplumbite refinement is therefore an averaged refinement, much like ones frequently met in order-disorder problems in crystal structures where more than one atomic species occupies one atomic site on the average.

Table 5, which lists the Pb–O distances, offers a possible explanation. The Pb–O ranges from 2.64 to 3.24 Å, a spread of 0.60 Å! In Ba[$Fe_{12}O_{19}$], the spread is 0.08 Å. This difference can be easily understood from the valence-shell electron-pair repulsion theory of Gillespie (1972). The longest Pb–O distances are across the (pseudo) invariant point at (⅔, ⅓, ¼) whereas the shortest Pb–O distances are on the same side from the invariant point as the closer oxygen receptors. The five unique Pb–Pb distances for split Pb range from 0.28 to 0.61 Å. The longest distance is nearly an inversion through (⅔, ⅓, ¼) to form Pb–Pb$^{(10)}$. The Pb–X ≈ 0.6 Å distance in general is now pursued further.

Pb splitting

Single-crystal X-ray diffraction followed by refinement is the method of choice for investigating Pb in a crystal structure because Pb, with an atomic number of 82, is

TABLE 6. Refined structures with split Pb atoms

Type 1															
Magnetoplumbite			2	$PbFe_{12}O_{19}$				*H*	*P*6$_3$/*mmc*		Pb–O 2.64–3.11 Å			Pb–Pb$^{(10)}$ 0.61(5) Å	
6	12*j*	*m*	⅙	Pb	0.722	0.371	¼		2*d*	$\bar{6}m2$	⅔	⅓	¼	*R* = 0.041 This study	
Beudantite			3	$PbFe_3(OH)_6(AsO_4)(SO_4)$				*R*	R$\bar{3}$*m*		Pb–O 2.64–3.10 Å			Pb–Pb′ 0.56 Å	
6	18*f*	2	⅙	Pb	0.038	0	0		3*a*	$\bar{3}m$	0	0	0	*R* = 0.037 Szymański (1988)	
Synthetic feldspar			4	$(Pb_{0.77}K_{0.23})(Si_{2.23}Al_{1.77}O_8)$				*M*	*C*2/*m*		Pb–O 2.54–3.65 Å			Pb–Pb′ 0.497(1) Å	
2	8*j*	1	½	$Pb_{0.77}$	0.275	0.019	0.143		4*i*	*m*	*x*	0	*z*	Pb–K 0.517(4) Å	
1	4*i*	*m*	1	$K_{0.23}$	0.279	0	0.082		4*i*	*m*	*x*	0	*z*	*R* = 0.034 Moore et al. (unpublished)	
Kentrolite			4	$Pb_2Fe_2O_2(Si_2O_7)$				*O*	*Pnab*		Pb(1),Pb(2)–O 2.20–3.41 Å			Pb(1)–Pb(2) 0.561(5) Å	
1	8*d*	1	0.77	Pb(1)	0.451	0.199	0.548		8*d*	1	*x*	*y*	*z*	*R* = 0.05 Moore et al. (unpublished)	
1	8*d*	1	0.23	Pb(2)	0.452	0.190	0.452		8*d*	1	*x*	*y*	*z*		
Type 2															
KPS			2	$Pb_2O(PbK)_2(Si_9O_{20})$				*Q*	*I*4/*mmm*		Pb(2)–O 2.49–3.47 Å			Pb(2)–K 0.59(1) Å	
1	8*i*	*mm*	½	Pb(2)	0.151	0.151	0		8*i*	*mm*	*x*	*x*	0	*R* = 0.034 Moore et al. (1985)	
1	8*i*	*mm*	½	K	0.186	0.186	0		8*i*	*mm*	*x*	*x*	0		
Hyalotekite			2	ca. $Pb_2Ba_2Ca_2(B_2Be_{0.5}Si_{9.5}O_{28})F$				*A*	*I*$\bar{1}$		Pb(1),Pb(2)–O 2.36–3.47 Å			Pb(1)–Ba(1) 0.439(8) Å	
1	4*i*	1	0.29	Pb(1)	0.154	0.173	0.004		4*i*	1	*x*	*y*	*z*	Pb(2)–Ba(2) 0.476(2) Å	
1	4*i*	1	0.71	Ba(1)	0.188	0.192	0.011		4*i*	1	*x*	*y*	*z*	*R* = 0.060 Moore et al. (1982)	
1	4*i*	1	0.29	Pb(2)	0.846	0.172	0.005		4*i*	1	*x*	*y*	*z*		
1	4*i*	1	0.71	Ba(2)	0.810	0.193	0.010		4*i*	1	*x*	*y*	*z*		
Joesmithite			2	$PbCa_2Mg_3Fe_2(OH)_2(Si_6Be_2O_{22})$				*M*	*P*2/*a*		Pb–O 2.56–3.49 Å			Pb–"A" 0.601(2) Å	
1	2*f*	2	1	Pb	¼	0.284	0		2*c*	$\bar{1}$	¼	¼	0(*C*2/*m*)	*R* = 0.13 Moore (1969, 1988)	

Note: Entries for type 1 along a row proceed as follows: name, cell formula, crystal system (*H* = hexagonal, *R* = rhombohedral, *M* = monoclinic, *O* = orthorhombic, *Q* = tetragonal or quadratic, *A* = triclinic or anorthic), space group, Pb–O distance range, splitting separation. The second row and, if present, third row continue as follows: atom coordinate(s), the same for coalesced position. Entries for type 2 are the same, except that the coalesced position is the same as the preceding entries in that row.

not only easily detected in compounds with a mean atomic number of ≈20, but the slightest perturbation of its position can be instantly detected in thermal-vibration anomalies. At least seven structure types are known to display split Pb positions, and these are summarized in Table 6. Several kinds of splittings are immediately evident. The Pb splitting is probably a complex problem. It is reminiscent of a related problem, that of several cation lone pairs (ψ) coordinated to a central cation as in magnussonite with its $(As^{3+}\psi)_6X$ cluster, where X is octahedrally coordinated by six lone pairs to form $[X\psi_6]$. Moore and Araki (1979) discussed this structure in considerable detail and provisionally proposed that $X = Mn^+$. A similar problem arose in dixenite with the tetrahedral cluster $(As^{3+}\psi)_4X$, $X = Cu^+$, discussed by Araki and Moore (1981) in some detail. In both structures, the As^{3+} sites are well-ordered, but the central X is split. In a way, this situation is the inverse of the splitting of a lone-pair cation such as Pb^{2+}.

From examining Table 6, it is evident that several kinds of splittings involving Pb^{2+} occur. The first type is self-splitting. Here, Pb^{2+} is split into several pieces. The cation may have moved from a Wyckoff position of low order to one of higher order. Included here are magnetoplumbite, beudantite, and synthetic feldspar. The equivalent sites of higher order appear to be each equally occupied. A subdivision of self-splitting is unequal population of Pb at two or more sites. This example is represented by kentrolite where about ¾Pb occurs at one site and ¼Pb at the other. The second type of splitting involves splitting of Pb^{2+} from a purported solid solution. Included here are synthetic feldspar (Pb-K splitting), joesmithite (Pb-Ca splitting?), KPS (Pb-K splitting), and hyalotekite (Pb-Ba splitting). Here the Pb-X splitting ranges from 0.44 to 0.60 Å. It is uncertain whether some Ca^{2+} remains at the "fixed" (¼, ¼, 0) site in joesmithite. Since the electron density would be relatively small, no extra atom position was recovered in this earlier study.

The second type of splitting can be readily explained, and this type was recently discussed in Moore (1988). Symmetry need not be broken at a site with at least one degree of freedom such as $\{C_n\}$ (n = 2, 3, 4, 6) rotation or $\{m\}$ reflection. Consider a solid solution of a cation with a lone electron pair and a cation stripped of all its valence electrons. For the former, there exists a lone pair–bond pair interaction in addition to bond pair–bond pair interaction, the latter which occurs solely for the stripped cation. This additional interaction forces some splitting

of the two ions with some change in an intensive parameter.

Many crystal structures are known for lead oxysalt minerals formed at low temperature. Roeblingite, a basic aquated plumbous calcium manganese sulfate cyclosilicate, is a typical example (Moore and Shen, 1984). Here $^{[7]}$Pb–O distances range from 2.22 to 3.42 Å. The range for $^{[7]}$Ca(2)–O is only 2.34 to 2.56 Å. Both are similar coordination polyhedra. The thermal parameter for Pb is B_{eq} = 1.04 Å^2 for this reasonably refined structure. The extensive range of Pb^{2+}–O distances is typical of crystals formed at low temperature. However, in Table 5, the Pb^{2+} splitting is indicative of crystals formed at high temperature such as synthetic magnetoplumbite, synthetic feldspar, synthetic KPS, and melanotekite. Temperatures of their formation were probably over 700 °C; the natural products are early skarn minerals. Beudantite, with a well-defined first-type splitting, has an unknown temperature of crystallization. This lack of data also applies to natural hyalotekite and joesmithite, with second-type splitting.

The *splitting index, P,* is defined as the ratio of the number of elements [*p*(a)] of the split Wyckoff atom position to the number of elements [*p*(b)] of the coalesced position of lower order. That is, $P = |p(a)|/|p(b)|$. The *p*(b) may or may not be a special invariant point. But on group-theoretical grounds, a *cascade* of splittings follows along Wyckoff positions of higher order, each splitting corresponding to an integral multiple of the equivalent point set of its lower-order predecessor. This cascade naturally limits those Wyckoff positions that are admissible for a given space group.

The cascade for magnetoplumbite in $P6_3/mmc$ would be

$$(2d)\ \bar{6}m2\ (\tfrac{2}{3}, \tfrac{1}{3}, \tfrac{1}{4}) \rightarrow (6h)\ mm\ (2x, x, \tfrac{1}{4}) \rightarrow (12j)\ m\ (x, y, \tfrac{1}{4}) \rightarrow (24l)\ (x, y, z).$$

Note that, in this study, the cascade terminates short of (24*l*), the Wyckoff general position that has no symmetry. Rather, it terminates at (12*j*) on the mirror plane at z = ¼, ¾. The split point has two degrees of freedom. That splitting may terminate at (6*h*) with one degree of freedom for a magnetoplumbite structure is not known. This Wyckoff position has two mutually orthogonal mirror planes. Are two mutually orthogonal mirror planes forbidden by the lone-pair effect? Again, no conclusion can be reached, although in Table 6, all cascades noted thus far converge to {*m*}, {2}, or {1} symmetry.

Consider structures studied at room temperature. For the minerals formed at low temperature, Pb^{2+} usually completely occupies at least one asymmetric atomic site. Crystal structures of these minerals tend to be rather unique. The Pb^{2+} oxysalts that formed at high temperature appear to show split Pb positions either of the first type or the second type. The explanation is not obvious, but we speculate that there exists a temperature, T_d, above which the Pb^{2+} cation is disordered. As such a phase is cooled from high temperature, T_d is traversed, the lone pair associated with Pb^{2+} emerges, and lone pair–bond pair interactions play a central role. Several pieces of evidence suggest this. Among other phases, matildite, $AgBiS_2$ has been long known to have an orthorhombic → cubic (galena-type) transition above 215 °C (Graham, 1951); study of both the quenched and high-temperature matildite structures would be most informative. An interesting speculation is that galena itself will evince some anomalous structural behavior either at room temperature or liquid-N_2 temperature. We envision that a lone pair–bond pair interaction, however small, could lead to splitting of Pb^{2+} from (4*a*) (0, 0, 0) to (32*f*) (*x, x, x*) in space group $Fm\bar{3}m$ with ⅛Pb^{2+} at a site in the latter position. In galena, the obvious manifestation of this would be found associated with a large isotropic thermal parameter. In many respects, an inverse of this type of problem was already discussed for magnussonite, which has purported [$As_6^{3+}Mn^+$] clusters. Six lone pairs point *toward* the central Mn. The central cation is split into six pieces, from (16*a*) (0, 0, 0) to (96*h*) (*x, y, z*) in space group *Ia*3*d*. The average distance from the refined general centroid of ⅙Mn^+ population to the invariant point is 0.46 Å (Moore and Araki, 1979). Since atom splittings and lone-pair effects have only recently been discussed, a lot of work remains to be done. Lone pairs in the service of geothermometry and geobarometry are virtually unexplored.

There is general good agreement between equivalent isotropic thermal parameters in this study on $PbFe_{12}O_{19}$ and that of Obradors et al. (1985) on $BaFe_{12}O_{19}$. The greatest difference is between Pb^{2+} (B = 1.50 Å^2) and Ba^{2+} (B = 0.57 Å^2). This difference, and perhaps the smaller differences for adjacent M(2) and O(3), probably arises from ⅙ Pb^{2+} occupancy and ensuing relatively high positional errors for (*x, y,* ¼) at position (12*j*). The possibility that several closely spaced Pb positions consequent to quenching may exist cannot be ruled out, however.

Although the mechanism behind splitting of lone-pair cations is barely understood, interactions between lone pair–bond pair effects and thermal vibration are consistent at least with a postulated T_d and the data at hand. Thermal vibration is responsive to temperature changes. In a study on pressure and temperature effects on the olivine structure, Hazen (1976) noted $B \approx 0.25$ Å^2 for octahedral M(1) and M(2) at 23 °C, which increased to $B \approx 1.2$ Å^2 at 675 °C on the same crystal. Since increased thermal effects promote increased disorder, it is logical to conclude that thermal vibration—lone pair–bond pair interaction—disorder are intimately connected. For this reason, study of certain structures—in particular wulfenite, $Pb^{2+}MoO_4$; galena, $Pb^{2+}S$; and KPS, $Pb_2O(Pb_2K_2)(Si_8O_{20})$—at high temperature is being considered.

Bond valences and Pb splitting

Brown (1981), in an extensive discussion on the valence-sum rule (in principle analogous to the famous Pauling electrostatic-valence rule), computed bond strength according to $s = (R/R_0)^{-N}$, where R is the determined bond length and R_0 and N are fitted constants. He included fitted constants for Pb^{2+}, Ba^{2+}, and Fe^{3+} in an appendix.

TABLE 7. Magnetoplumbite bond valences

Cations	Anions O(1)	O(2)	O(3)	O(4)	O(5)	Cation sum (→)	
Pb			O(3) + O(3)$^{(1)}$ 0.324 (×3)→ O(3)$^{(4)}$ + O(3)$^{(41)}$ 0.289 (×3)→ O(3)$^{(2)}$ + O(3)$^{(21)}$ 0.268 (×3)→ ×1↓		O(5)$^{(2)}$ 0.221 (×6)→ O(5) 0.158 (×6)→ O(5)$^{(4)}$ 0.121 (×6)→ ×1↓	2.30 1.82 1.53	(2.31)
Fe(1)				0.518 (×6)→ ×1↓		3.11	(3.09)
Fe(2)	0.350 (×1)→ ×½↓ 0.178 (×1)→ ×½↓		0.741 (×3)→ ×1↓			2.75	(2.80)
Fe(3)		0.721 (×1)→ ×1↓		0.713 (×3)→ ×1↓		2.86	(2.81)
Fe(4)			0.446 (×3)→ ×2↓		0.571 (×3)→ ×1↓	3.05	(2.95)
Fe(5)	0.557 (×1)→ ×3↓	0.403 (×1)→ ×3↓		0.386 (×2)→ ×2↓	0.659 (×2)→ ×2↓	3.05	(2.94)
	Anion sum (↓)						
	1.94	1.93	1.96 1.92 1.90	2.00	2.11 2.05 2.01		
	(1.87)	(1.90)	(1.95)	(1.97)	(2.03)		

Note: Bond valences and multiplicities show horizontal arrows for cation-valence sums and vertical arrows for anion-valence sums. Note splitting of O(3) into three O(3) + O(3)′ pairs and O(5) into three O(5) pairs. The valence sums of Obradors et al. (1985) are in parentheses, and the general outline of our Table 6 follows their study. See Table 4 for equipoint designations.

We effectively repeated the procedure used by Obradors et al. (1985) who used the same method. The Pb^{2+} is coordinated by O(3) and O(5). Our Pb^{2+} is split into six pieces, however. That means for fixed Pb^{2+}, six distinct O(3) and three distinct O(5) pairs exist. The first six correspond to equatorial bonds of the type O(3) + O(3)(t) where t is a cell translation, and the second three are apical bonds of the type O(5). All Pb–O(3,5) bonds are included in Table 5.

The bond valences for all cations and anions in our magnetoplumbite appear in Table 7. The findings of Obradors et al. (1985) are listed parenthetically for comparative purposes. The agreement is very good between the two studies. It is seen that the differences arising from three types of O(3) and three types of O(5) bonds are too small to admit any conclusions. We also calculated bond-valence sums by fixing Pb^{2+} at (⅔, ⅓, ¼), keeping all other atoms in their refined positions. The calculated Pb–O distances (compared with Ba–O of Obradors et al. (1985) in parentheses) are 6Pb–O(3) 2.942 (2.950) and 6Pb–O(5) 2.839 (2.868) Å. Bond-valence sums now become 1.93 for Pb, 1.90 for O(3), and 2.08 for O(5), within the range of values in Table 7.

The lone pair–bond pair interaction clearly has many interesting implications. The nature of the problem requires a large data set of high-quality reflections, the data preferably collected on small spheres owing to high linear atomic absorption. The possibility of harnessing lone pairs as geothermometers and geobarometers will require more reconnaissance work. Perhaps many "old" structure studies will have to be re-evaluated. Sulfosalts, in particular, will need some re-examination. The possibility that lone-pair cations such as Tl^{+}, Pb^{2+}, Bi^{3+}, Sb^{3+}, and As^{3+} segregate and accumulate over a long period of geologic time is yet another tantalizing prospect in economic geology. For a while at least, it is anticipated that lone-pair cations will be greeted with some skepticism, disbelief, and indifference by the earth sciences community.

ACKNOWLEDGMENTS

The synthetic magnetoplumbite was a serendipitous find, and we thank Mr. John S. White, Jr., and Dr. Kurt Nassau for their help.

P.B.M. acknowledges support by the National Science Foundation (grant EAR 87-07382), and P.K.S. thanks the Tennessee Earthquake Information Center for use of their VAX computer.

REFERENCES CITED

Aminoff, G. (1925) Über ein neues oxydisches Mineral aus Långban (Magnetoplumbit). Geologiska Föreningens i Stockholm Förhandlingar, 47, 283–289.

Araki, T., and Moore, P.B. (1981) Dixenite: Metallic $[As_4^{3+}Cu^{1+}]$ clusters in an oxide matrix. American Mineralogist, 66, 1263–1273.

Brown, I.D. (1981) The bond valence method: An empirical approach to chemical structure and bonding. In M. O'Keeffe and A. Navrotsky, Eds., Structure and bonding in crystals, vol. 2, p. 1–30. Academic Press, New York.

Cromer, D.T., and Olsen, C.E. (1959) The crystal structures of $PuNi_3$ and $CeNi_3$. Acta Crystallographica, 12, 689–694.

Gillespie, R.J. (1972) Molecular geometry. Van Nostrand–Reinhold, London.

Graham, A.R. (1951) Matildite, aramayoite, miargyrite. American Mineralogist, 36, 436–449.

Grey, I.E., Madsen, I.C., and Haggerty, S.E. (1987) Structure of a new

upper-mantle, magnetoplumbite-type phase. American Mineralogist, 72, 633–636.

Hazen, R.M. (1976) Effects of temperature and pressure on the crystal structure of forsterite. American Mineralogist, 61, 1280–1293.

Ibers, J.A., and Hamilton, W.C., Eds. (1974) International tables for X-ray crystallography, vol. 4, p. 99–100. Kynoch Press, Birmingham, England.

Moore, P.B. (1969) Joesmithite: A novel amphibole crystal chemistry. Mineralogical Society of America Special Paper 2, 111–115.

——— (1973) Bracelets and pinwheels: A topological-geometrical approach to the calcium orthosilicate and alkali sulfate structures. American Mineralogist, 58, 32–42.

——— (1988) The joesmithite enigma: Note on the $6s^2Pb^{2+}$ lone pair. American Mineralogist, 73, 843–844.

Moore, P.B., and Araki, T. (1979) Magnussonite, manganese arsenite, a fluorite derivative structure. American Mineralogist, 64, 390–401.

Moore, P.B., and Shen, J. (1984) Roeblingite: Its crystal structure and comments on the lone pair effect. American Mineralogist, 69, 1173–1179.

Moore, P.B., Araki, T., and Ghose, S. (1982) Hyalotekite, a complex lead borosilicate: Its crystal structure and the lone-pair effect of Pb(II). American Mineralogist, 67, 1012–1020.

Moore, P.B., Sen Gupta, P.K., and Schlemper, E.O. (1985) Solid solution in plumbous potassium oxysilicate affected by interaction of a lone pair with bond pairs. Nature, 318, 548–550.

Moore, P.B., Schlemper, E.O., and Sen Gupta, P.K. (1989) Kornerupine: Chemical crystallography, comparative crystallography and its relation to olivine and Ni_2In intermetallic. American Mineralogist, 74, 642–655.

Obradors, X., Collomb, A., Pernet, M., Samaras, D., and Joubert, J.C. (1985) X-ray analysis of the structural and dynamic properties of $BaFe_{12}O_{19}$ hexagonal ferrite at room temperature. Journal of Solid State Chemistry, 56, 171–181.

Szymański, J.T. (1988) The crystal structure of beudantite, $Pb(Fe,Al)_3[(As,S)O_4]_2(OH)_6$. Canadian Mineralogist, 26, 923–932.

Townes, W.D., Fang, J.H., and Perrotta, A.J. (1967) The crystal structure and refinement of ferrimagnetic barium ferrite, $BaFe_{12}O_{19}$. Zeitschrift für Kristallographie, 125, 437–449.

Villars, P., and Calvert, L.D. (1985) Pearson's handbook of crystallographic data for intermetallic phases, vols. 1–3. American Society for Metals, Metals Park, Ohio, 3258 p.

Manuscript received November 30, 1988
Manuscript accepted June 2, 1989